

Electronic excitation of H₂O by electron impact

M-T Lee†, S E Michelin‡, T Kroin‡, L E Machado§ and L M Brescansin||

† Departamento de Química, Universidade Federal de São Carlos, 13565-905, São Carlos, SP, Brazil

‡ Departamento de Física, Universidade Federal de Santa Catarina, 88049 Florianópolis, SC, Brazil

§ Departamento de Física, Universidade Federal de São Carlos, 13565-905, São Carlos, SP, Brazil

|| Instituto de Física 'Gleb Wataghin', UNICAMP, 13083-970, Campinas, SP, Brazil

Received 17 January 1995

Abstract. Recently we made calculations of differential and integral cross sections for the $X^1A_1 \rightarrow {}^3A_1(3a_1 \rightarrow 3sa_1)$ transition in H₂O in the energy range of 12–30 eV, where the distorted-wave approximation was applied for the first time to study the electronic excitation of a nonlinear polyatomic target by electron impact. In the present work we make an extension of this calculation for that transition to the energy range 40–150 eV. Calculations of cross sections for the $X^1A_1 \rightarrow {}^3A_1(3a_1 \rightarrow 3pa_1)$ transition in the energy range 14–150 eV are also reported. The present study is the first theoretical investigation of electron-impact excitation of the channel $3a_1 \rightarrow 3pa_1$ in this nonlinear molecule.

1. Introduction

Electronic excitation cross sections of atoms and molecules are of fundamental importance in a great variety of physical and chemical processes and constitute a subject of continuously increasing interest to both experimentalists and theoreticians working in this field (Trajmar *et al* 1983). However, measurements of electron-impact excitation cross sections are, in general, difficult and up to now the reported results in the literature have been fragmentary and, in some cases, there are major discrepancies among various experimental data (Trajmar *et al* 1983, Collins and Schneider 1990). In this sense, the development of theoretical methods leading to reliable cross sections is desirable as a support for the interpretation of experimental measurements, as well as for providing information on cross sections whose experimental determination is especially complex. Recently, several solid-based *ab initio* multichannel theories have been developed for the treatment of elastic and inelastic electron-molecule collisions (Lima *et al* 1988, Branchett *et al* 1990, 1991, Parker *et al* 1991). Although these methods have a very firm theoretical basis, computationally they are still reasonably difficult to apply. Thus, their applications to the inelastic e^- -molecule scattering have been restricted to a few molecular targets and even for a small target such as H₂ only a few channels have been explicitly included in the calculations. Recent theoretical studies (Parker *et al* 1991, Branchett *et al* 1990, 1991) have shown that multichannel effects are important in the calculation of the low-energy electron-impact excitation cross sections, particularly for the H₂(X) \rightarrow H₂(c) transition. Nevertheless, the calculated results of differential and integral excitation cross sections using different multichannel methods show significant discrepancies (Parker *et al* 1991, Branchett and Tennyson 1990, Branchett *et*

et al 1990, 1991), indicating that more systematic studies will be needed on this subject. On the other hand, over the past two decades several low-order theories such as the Born and Ochkur–Rudge approximations (Cartwright and Kuppermann 1967, Chung *et al* 1975, Chung and Lin 1978), the impact parameter method (Hazi 1981), and distorted-wave approximations (DWA, Rescigno *et al* 1974, Fliflet and McKoy 1980, Lee and McKoy 1983, Lee *et al* 1990a, b, 1991) have been applied to study inelastic electron scattering associated with the electronic excitation of molecules. These theories are computationally easier to apply and can provide useful results in some applications. Particularly, the DWA (Bartschat and Madison 1987) and first-order many-body theory (FOMBT, Meneses *et al* 1990), which is essentially equivalent to DWA, have been successfully and widely applied to calculate electronic excitation cross sections and coherence parameters for atomic targets in the intermediate and high energy ranges. The validity of DWA for molecular targets has been discussed recently by Lee *et al* (1990a), where the DWA calculations of the electron-impact excitation cross sections for the three first triplet excited states of H_2 have led to similar results to those obtained with the two-state Schwinger multichannel method (SMC, Lima *et al* 1988) even for incident energies a few eV above threshold. These studies suggested that the DWA could be adequate for studies of electronic excitation of molecules by electron impact in the intermediate energy range.

More recently, experimental results of electron-excitation cross sections for CO in the energy range 20–50 eV (Middleton *et al* 1993) have revealed a good agreement with DWA theory, both in shape and magnitude, particularly for the incident energy of 50 eV. The applicability of DWA has been recently extended to study the excitation of a nonlinear target by electron impact. Specifically, inelastic differential and integral cross sections for the transition $X^1A_1 \rightarrow {}^3A_1(3a_1 \rightarrow 3sa_1)$ of H_2O in the 12–30 eV range were reported (Lee *et al* 1993). In this paper we extend the application of DWA to calculate electronic excitation cross sections associated with the transitions $X^1A_1 \rightarrow {}^3A_1(3a_1 \rightarrow 3sa_1)$ and $X^1A_1 \rightarrow {}^3A_1(3a_1 \rightarrow 3pa_1)$ in H_2O for incident energies ranging from near threshold to 150 eV. Our purpose is to provide electronic excitation cross sections in the intermediate energy range, since there is a lack of such data in the literature.

2. Theory

The details of the basic theory used in the present work have already been presented elsewhere for linear molecules (Rescigno *et al* 1974, Fliflet and McKoy 1980, Lee and McKoy 1983, Lee *et al* 1990a, b, 1991) and will be only briefly described here. Differential excitation cross sections for electron–molecule scattering are given by

$$\frac{d\sigma}{d\Omega} = \frac{1}{8\pi^2} \int d\alpha \sin \beta d\beta d\gamma |f(\hat{k}_i, \hat{k}_f)|^2 \quad (1)$$

where $f(\hat{k}_i, \hat{k}_f)$ is the laboratory-frame (LF) scattering amplitude, \hat{k}_i and \hat{k}_f are the directions of incident and scattered electron linear momenta, respectively, and (α, β, γ) are the Euler angles which define the direction of the molecular principal axis. The body-frame (BF) amplitude $f(\hat{k}_i, \hat{k}_f)$ is related to the T -matrix elements by the formula

$$f(\hat{k}_i, \hat{k}_f) = -2\pi^2 T_{if}. \quad (2)$$

In the DWA, the transition T -matrix is given by

$$T_{if} = \langle \varphi_1 \Psi_{k_f} | U_{se} | \varphi_0 \Psi_{k_i} \rangle \quad (3)$$

where φ_0 and φ_1 are the initial and final target wavefunctions, respectively. These wavefunctions are Slater determinants with appropriate symmetries. The Ψ_{k_i} and Ψ_{k_f} are the

initial and final distorted continuum wavefunctions and U_{se} is the static-exchange potential operator. These distorted wavefunctions are solutions of the Lippmann–Schwinger equation:

$$\Psi_k^{(\pm)} = \Phi_k + G_0^{(\pm)} U \Psi_k^{(\pm)} \quad (4)$$

with $G_0^{(\pm)}$ being the free-particle Green's operator with outgoing ($G_0^{(+)}$) or incoming ($G_0^{(-)}$) wave boundary conditions, and Φ_k is a plane wavefunction, with linear momentum \mathbf{k} . These wavefunctions Ψ_k were calculated using the Schwinger variational iterative method (SVIM) (Lucchese *et al* 1982) in the static-exchange field of the ground-state target. These continuum wavefunctions are single-centre expanded as

$$\Psi_k(\mathbf{r}) = (2/\pi)^{1/2} \sum_{p\mu lh} \frac{(i)^l}{k} \Psi_{klh}^{p\mu}(\mathbf{r}) X_{lh}^{p\mu*}(\hat{\mathbf{k}}) \quad (5)$$

where $X_{lh}^{p\mu}(\hat{\mathbf{k}})$ are symmetry-adapted functions which are related to the usual spherical harmonics by

$$X_{lh}^{p\mu}(\hat{\mathbf{r}}) = \sum_m b_{lhm}^{p\mu} Y_{lm}(\hat{\mathbf{r}}) \quad (6)$$

and satisfy well known orthonormality relations (Burke *et al* 1972). The coefficients $b_{lhm}^{p\mu}$ for the point group C_{2v} are given by Burke *et al* (1972). In equation (6) p is one of the irreducible representations (IR) of the molecular point group, μ is a component of this representation, and h distinguishes between different bases for the same IR corresponding to the same value of l .

The calculation of $\Psi_k(\mathbf{r})$ starts with the expansion of the trial functions in a set R_0 of L^2 basis functions $\alpha_i(\mathbf{r})$ as follows:

$$\tilde{\Psi}_{k,lh}^{p\mu}(\mathbf{r}) = \sum_{i=1}^N a_{i,lh}^{p\mu}(k) \alpha_i(\mathbf{r}). \quad (7)$$

Using this basis set, the reactance K -matrix elements can be derived as

$$K_{k,lh;l'h'}^{p\mu(R_0)} = \sum_{i,j=1}^N \langle \Phi_{k,lh}^{p\mu} | U | \alpha_i \rangle [D]_{ij}^{-1} \langle \alpha_j | U | \Phi_{k,lh}^{p\mu} \rangle \quad (8)$$

where

$$D_{ij} = \langle \alpha_i | U - U G_0^{(P)} U | \alpha_j \rangle. \quad (9)$$

Here $G_0^{(P)}$ is the principal value of the free-particle Green's operator and the zeroth-iteration wavefunction $\Psi_{k,lh}^{(R_0)}$ is calculated using (7) with appropriately calculated coefficients $a_{i,lh}^{p\mu}$. As in the case of linear molecules (Lucchese *et al* 1982), converged solutions of (4) can be obtained via an iterative procedure. The method consists in augmenting the basis set R_0 by the set

$$S_0 = \left\{ \Psi_{k,l_1 h_1}^{(-)p\mu(R_0)}(\mathbf{r}), \Psi_{k,l_2 h_2}^{(-)p\mu(R_0)}(\mathbf{r}), \dots, \Psi_{k,l_c h_c}^{(-)p\mu(R_0)}(\mathbf{r}) \right\} \quad (10)$$

where l_c is the maximum value of l for which the expansion (5) of the scattering solution is truncated, and $h_c \leq l_c$. A new set of partial wave scattering solutions can now be obtained from

$$\Psi_{k,lh}^{(+)p\mu(R_1)}(\mathbf{r}) = \Phi_{k,lh}^{p\mu}(\mathbf{r}) + \sum_{i,j=1}^M \langle \mathbf{r} | G^{(+)} U | \eta_i^{(R_1)} \rangle [D^{(+)}]_{ij}^{-1} \langle \eta_j^{(R_1)} | U | \Phi_{k,lh}^{p\mu} \rangle \quad (11)$$

where $\eta_i^{(R_1)}(\mathbf{r})$ is any function in the set $R_1 = R_0 \cup S_0$ and M is the number of functions in R_1 . This iterative procedure continues until a converged $\Psi_{k,lh}^{(+),p\mu(R_n)}(\mathbf{r})$ is achieved after the n th iteration.

Using these converged wavefunctions, the T -matrix can be partial-wave expanded as

$$T_{if} = (2/\pi) \sum_{p\mu lh} \sum_{p'l'\mu'h'} \frac{i^{l-l'}}{k_i k_f} T_{lh'l'h'}^{p\mu p'\mu'} X_{lh}^{p\mu*}(\hat{k}_i) X_{l'h'}^{p'\mu'}(\hat{k}_f) \quad (12)$$

where $T_{lh'l'h'}^{p\mu p'\mu'}$ is the partial T -matrix element given by

$$T_{lh'l'h'}^{p\mu p'\mu'} = \langle \varphi_1 \Psi_{k_i, l'h'}^{p'\mu'} | U_{se} | \varphi_0 \Psi_{k_i, lh}^{p\mu} \rangle. \quad (13)$$

For the transition studied herein, only the exchange part of the T -matrix is needed. Finally, the laboratory-frame differential cross section (DCS) is represented in a j_i basis (Fano and Dill 1972) as

$$\frac{d\sigma}{d\Omega} = \frac{3}{2} \frac{k_f}{k_i} \sum_{j_i m_i m_{i'}} \frac{1}{(2j_i + 1)} |B_{m_i m_{i'}}^{j_i}|^2 \quad (14)$$

where $j_i = l' - l$ is the transferred angular momentum during the collision, $m_{i'}$ and m_i are the projections of j_i along the laboratory and molecular axis, respectively, and the j_i -basis dynamic coefficients $B_{m_i m_{i'}}^{j_i}$ are given by

$$B_{m_i m_{i'}}^{j_i} = \sum_{p' p \mu' \mu l' l h' h m' m} i^{l-l'} (2l' + 1)^{1/2} (-1)^{m'} b_{lh}^{p\mu} b_{l'h'}^{p'\mu'} \times \langle l'l' 0 m_i | j_i m_i \rangle \langle l'l' - m m' | j_i m_{i'} \rangle T_{lh'l'h'}^{p\mu p'\mu'} Y_{l'm_i}(\hat{k}_f) \quad (15)$$

where the elements $\langle l_1 l_2 m_1 m_2 | LM \rangle$ are the Clebsch-Gordan coefficients, and the Y_{lm} are the usual spherical harmonics.

3. Computational details

In the DWA, the initial and final wavefunctions of the scattering electron, needed for the computation of the T -matrix, were obtained in the ground-state molecular potential field in the static-exchange level. Both ground and excited target wavefunctions φ_0 and φ_1 were calculated using the [3s2p, 2s] contracted basis set of Dunning and Hay (1977), augmented by three s ($\alpha = 0.112, 0.055$ and 0.016), one p ($\alpha = 0.065$), and two d ($\alpha = 1.322$ and 0.3916) uncontracted functions on oxygen and one uncontracted p function ($\alpha = 1.12$) on the hydrogens, for the $X^1A_1 \rightarrow {}^3A_1(3a_1 \rightarrow 3sa_1)$ transition. For the $X^1A_1 \rightarrow {}^3A_1(3a_1 \rightarrow 3pa_1)$ transition the initial basis set of Dunning and Hay (1977) was augmented by three s ($\alpha = 0.192, 0.115$ and 0.016), one p ($\alpha = 0.065$), and two d ($\alpha = 0.955$ and 0.5316) uncontracted functions on oxygen and one uncontracted p function ($\alpha = 1.12$) on the hydrogens. At the experimental equilibrium geometry, $R_{O-H} = 1.8085 a_0$ and $\theta_{H-O-H} = 104.5^\circ$, these two basis sets led to the same SCF energy of -76.048 au, compared with the Hartree-Fock limit of -76.066 au (Dunning *et al* 1972). The wavefunctions of the excited states were calculated using the improved virtual orbital (IVO) approximation. The calculated vertical excitation energies for the $X^1A_1 \rightarrow {}^3A_1(3a_1 \rightarrow 3sa_1)$ and $X^1A_1 \rightarrow {}^3A_1(3a_1 \rightarrow 3pa_1)$ transitions are 10.35 and 13.33 eV, respectively, values to be compared with 10.21 eV from Pritchard *et al* (1990) and 12.1 eV from Schaeffer (1977).

In order to ensure convergence of all angular momentum expansions, terms up to $l_{\max} = 7$ were included for each symmetry in the energy range 12–90 eV, and up to

$l_{\max} = 11$ for the energy range 100–150 eV. We have verified that the contribution from higher-order partial waves to the DCS is less than 2% for the impact energies considered in this work. All results presented here converged within five iterations.

4. Results

Figures 1 and 2 show the integral cross sections (ICS) for the excitations $X^1A_1 \rightarrow {}^3A_1(3a_1 \rightarrow 3sa_1)$ and $X^1A_1 \rightarrow {}^3A_1(3a_1 \rightarrow 3pa_1)$, respectively, at impact energies (E_0) ranging from near threshold to 150 eV. The behaviour of the ICS in the low-energy region is shown in detail in the insets of both figures. For the $X^1A_1 \rightarrow {}^3A_1(3a_1 \rightarrow 3sa_1)$ transition, relative emission measurements (Becker *et al* 1980), normalized to our results at 30 eV and SMC results (Pritchard *et al* 1990) are also shown in the inset for comparison. It can be seen that the position of the maximum of the ICS (around 16 eV) is well reproduced by both theories. However, the minimum below 15 eV, predicted by both calculations, is not observed experimentally. Above 20 eV, the ICS for both transitions decrease rapidly but smoothly with increasing incident energies. Unfortunately, the lack of experimental and theoretical data in the energy range above 30 eV makes their comparison with the present results impossible, thus seriously limiting the discussion.

In figures 3 and 4 we show the DCS for the $X^1A_1 \rightarrow {}^3A_1(3a_1 \rightarrow 3sa_1)$ excitation by electron impact in the 12–30 and 30–120 eV ranges, respectively. Data for some selected energies are also shown in table 1. At lower energies, the structure of DCS as a function of incident energies is similar to that seen in the ICS curve. Furthermore, the angular distribution of the DCS at incident energies near threshold is closely isotropic, reflecting

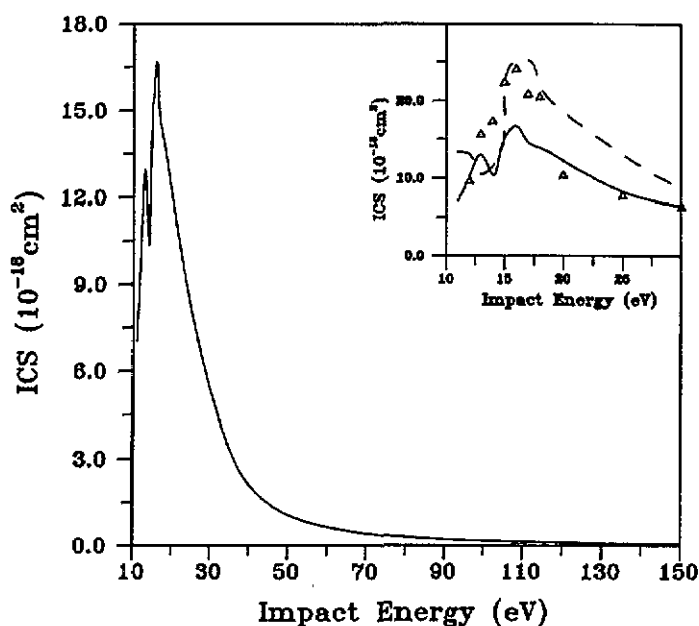


Figure 1. Integral cross sections for electron-impact excitation $X^1A_1 \rightarrow {}^3A_1(3a_1 \rightarrow 3sa_1)$ in H_2O . Full curve, present iteratively converged results; broken curve, two-state SMC results of Pritchard *et al* (1990); triangles, relative emission measurements of Becker *et al* (1980) normalized to our calculated results at 30 eV.

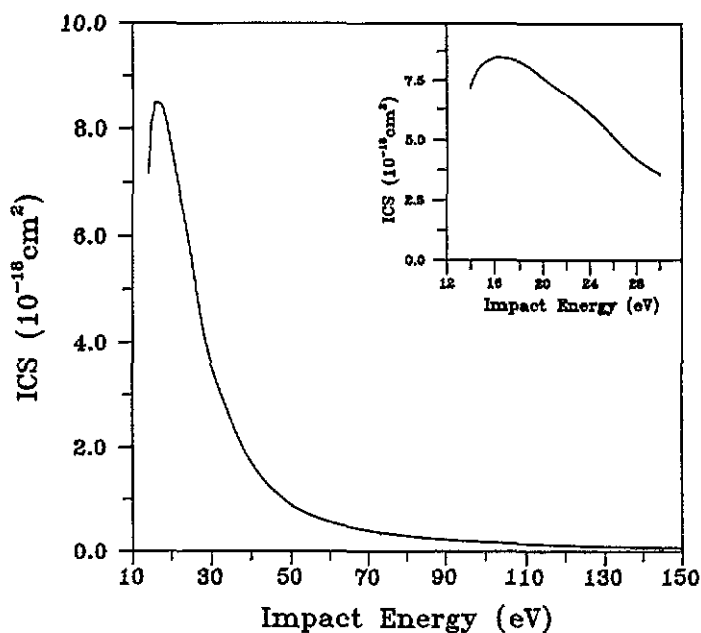


Figure 2. Same as figure 1 for $X^1A_1 \rightarrow ^3A_1(3a_1 \rightarrow 3p_{a_1})$ excitation.

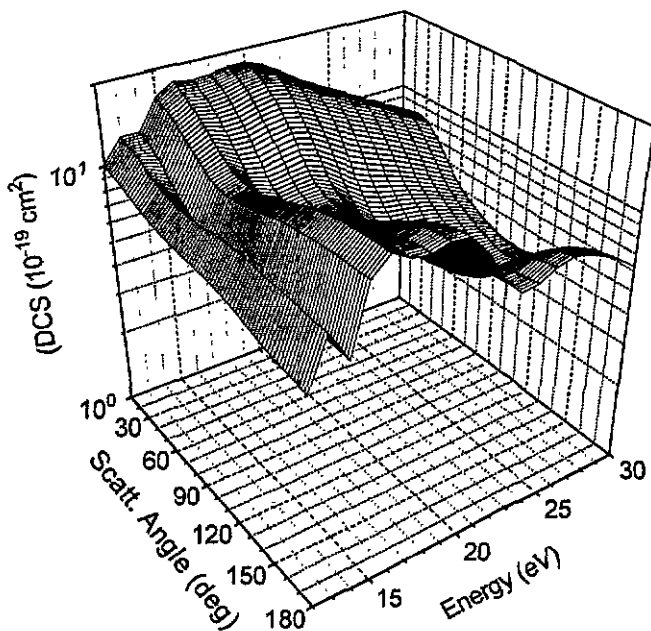


Figure 3. Differential cross sections for electron-impact excitation $X^1A_1 \rightarrow ^3A_1(3a_1 \rightarrow 3s_{a_1})$ in H_2O at lower incident energies.

the dominant contribution of the s-wave to the cross sections. With the increase of the incident energies, contributions of higher partial waves become important. Therefore, in

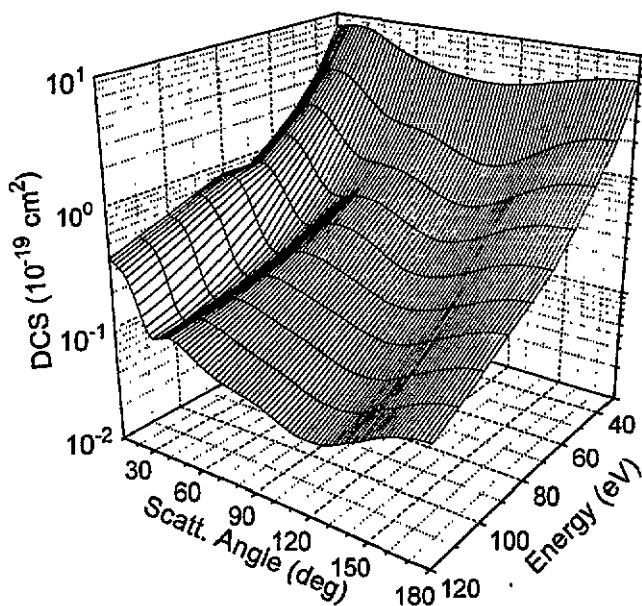


Figure 4. Same as figure 3, for higher energies.

Table 1. DCS and ICS (in 10^{-19} cm^2) for the excitation $X^1A_1 \rightarrow {}^3A_1(3a_1 \rightarrow 3sa_1)$ in H₂.

Angle (deg)	E_0 (eV)						
	12	20	25	30	50	100	120
10	10.08	17.75	11.58	7.64	1.82	0.544	0.376
20	9.79	17.38	12.05	8.22	2.15	0.455	0.290
30	9.39	16.25	11.71	8.06	1.83	0.193	0.124
40	8.97	14.35	10.40	7.12	1.22	0.139	0.113
50	8.62	12.29	8.69	6.02	0.888	0.154	0.109
60	8.36	10.35	7.21	5.20	0.835	0.145	0.088
70	8.22	9.13	6.15	4.68	0.832	0.128	0.073
80	8.16	8.53	5.43	4.33	0.773	0.113	0.065
90	8.12	8.41	4.92	4.11	0.665	0.101	0.059
100	8.04	8.61	4.57	3.99	0.563	0.087	0.050
110	7.90	9.04	4.42	4.03	0.514	0.077	0.043
120	7.69	9.66	4.54	4.22	0.536	0.073	0.041
130	7.42	10.43	4.99	4.54	0.625	0.073	0.043
140	7.12	11.31	5.72	4.96	0.771	0.091	0.052
150	6.85	12.19	6.60	5.41	0.950	0.111	0.062
160	6.62	12.97	7.43	5.83	0.111	0.134	0.076
170	6.48	13.49	8.01	6.13	0.121	0.155	0.085
180	6.43	13.68	8.22	6.24	0.126	0.165	0.089
ics	101.6	122.2	82.5	54.6	10.7	1.63	1.00

the 15–30 eV range, a minimum around 90° is clearly shown up. For higher energies two minima at about 45° and 120°, which reflect the d-wave contribution, are seen.

Figures 5 and 6 show the DCS for the $X^1A_1 \rightarrow {}^3A_1(3a_1 \rightarrow 3pa_1)$ transition in the 14–30 eV and 30–120 eV ranges, respectively. Again, cross sections for some selected energies are also shown in table 2. For this transition, the energy dependence of the angular distribution

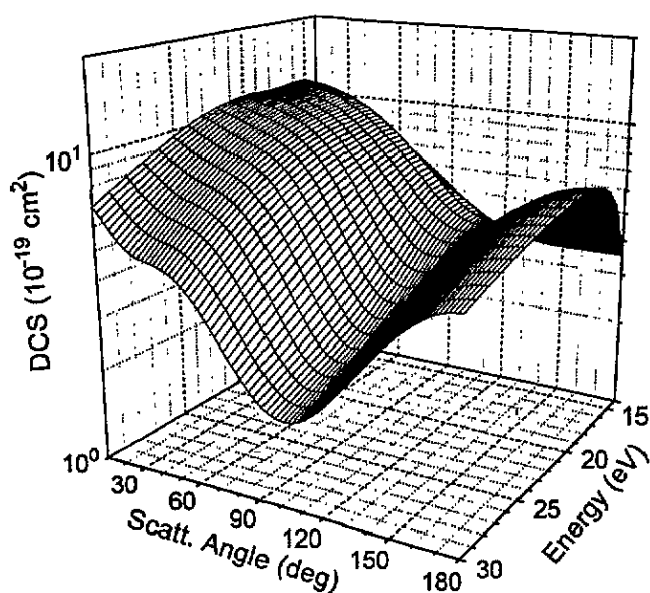


Figure 5. Same as figure 3, for the $X^1A_1 \rightarrow {}^3A_1(3a_1 \rightarrow 3pa_1)$ excitation.

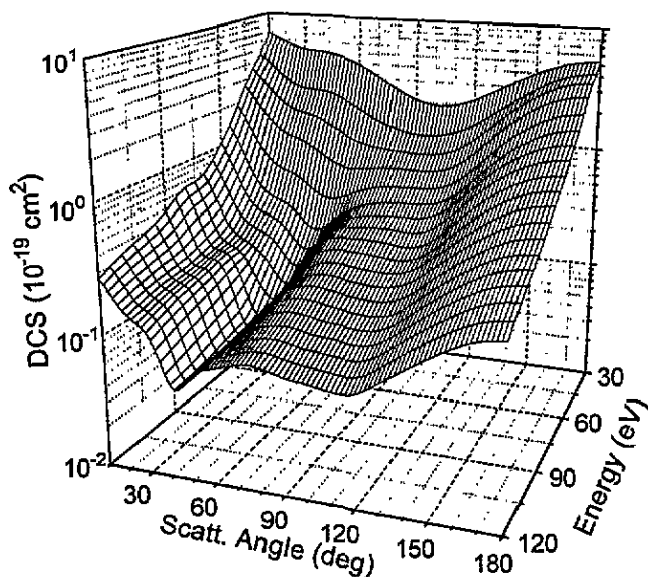


Figure 6. Same as figure 5, for higher energies.

of the DCS is essentially similar to that of the $X^1A_1 \rightarrow {}^3A_1(3a_1 \rightarrow 3sa_1)$ excitation except near threshold, where the DCS for $X^1A_1 \rightarrow {}^3A_1(3a_1 \rightarrow 3pa_1)$ transition is more forward enhanced.

Unfortunately, there are not yet enough calculated or experimental DCS for the excitations studied herein to compare with. However, previously reported DWA results for a few other molecules (Rescigno *et al* 1974, Lee and Mckoy 1983, Lee *et al* 1990a) have shown

Table 2. DCS and ICS (in 10⁻¹⁹ cm²) for the excitation $X^1A_1 \rightarrow {}^3A_1(3a_1 \rightarrow 3p_{a_1})$ in H₂.

Angle (deg)	E_0 (eV)						
	14	20	25	30	50	100	120
10	10.14	11.28	9.57	6.90	1.91	0.394	0.269
20	9.84	10.87	8.75	5.75	1.01	0.199	0.162
30	9.36	10.37	8.12	5.07	0.623	0.153	0.116
40	8.75	9.79	7.70	4.86	0.527	0.060	0.049
50	8.03	8.96	7.08	4.53	0.397	0.065	0.061
60	7.26	7.80	6.05	3.89	0.350	0.095	0.073
70	6.49	6.42	4.80	3.14	0.411	0.119	0.083
80	5.76	5.07	3.62	2.51	0.471	0.126	0.083
90	5.10	4.03	2.78	2.08	0.498	0.118	0.075
100	4.56	3.47	2.41	1.91	0.504	0.112	0.071
110	4.13	3.43	2.51	1.97	0.513	0.109	0.066
120	3.83	3.83	2.97	2.23	0.588	0.119	0.069
130	3.64	4.50	3.66	2.68	0.800	0.157	0.088
140	3.54	5.27	4.42	3.28	1.16	0.214	0.115
150	3.51	5.99	5.15	3.95	1.61	0.280	0.147
160	3.51	6.57	5.76	4.60	2.06	0.352	0.184
170	3.52	6.94	6.16	5.08	2.40	0.410	0.215
180	3.53	7.07	6.31	5.26	2.52	0.432	0.227
ics	71.7	76.0	56.2	35.7	8.92	1.83	1.16

that this approximation is able to reproduce at least the shape of the DCS for energies starting from a few eV above threshold. In addition, quantitative agreement of DWA results with experimental data was also observed for energies in the intermediate energy region (Middleton *et al* 1993). In this sense, the present results above 30 eV are expected to be quantitatively reliable. Considering the scarceness of the experimental data, it is hoped that our work can stimulate further developments in molecular excitation experiments and then serve as comparison with the results obtained.

Acknowledgments

The authors would like to thank Evandro M S Ribeiro for his careful preparation of the figures. This research was partially supported by Brazilian agencies Conselho Nacional de Desenvolvimento Científico e Tecnológico (CNPq), FAPESP and FINEP-PADCT.

References

- Bartschat K and Madison D H 1987 *J. Phys. B: At. Mol. Phys.* **20** 5839
- Becker K H, Stumpf B and Schultz G 1980 *Chem. Phys. Lett.* **73** 102
- Branchett S E, Tennyson J and Morgan L A 1990 *J. Phys. B: At. Mol. Opt. Phys.* **23** 4625
- 1991 *J. Phys. B: At. Mol. Opt. Phys.* **24** 3479
- Burke P G, Chandra N and Thompson G N 1972 *J. Phys. B: At. Mol. Phys.* **5** 1696
- Cartwright D C and Kuppermann A 1967 *Phys. Rev.* **163** 86
- Chung S and Lin C C 1978 *Phys. Rev. A* **17** 1874
- Chung S, Lin C C and Lee E T P 1975 *Phys. Rev. A* **12** 1340
- Collins L A and Schneider B I 1990 *Electronic and Atomic Collisions* ed H B Gilbody, W R Newell, F H Read and A C H Smith (Amsterdam: Elsevier)
- Dunning T H Jr and Hay J P 1977 *Modern Theoretical Chemistry* vol 3 (New York: Plenum) p 1
- Dunning T H Jr, Pitzer R M and Aung S 1972 *J. Chem. Phys.* **57** 5044

- Fano U and Dill D 1972 *Phys. Rev. A* **6** 185
- Fliflet A W and McKoy V 1980 *Phys. Rev. A* **21** 1863
- Hazi A U 1981 *Phys. Rev. A* **23** 2232
- Lee M-T, Brescansin L M and Lima M A P 1990a *J. Phys. B: At. Mol. Opt. Phys.* **23** 3859
- Lee M-T, Machado L E, Brescansin L M and Meneses G D 1991 *J. Phys. B: At. Mol. Opt. Phys.* **24** 509
- Lee M-T, Machado L E, Leal E P, Brescansin L M, Lima M A P and Machado F B C 1990b *J. Phys. B: At. Mol. Opt. Phys.* **23** L233
- Lee M-T and McKoy V 1983 *Phys. Rev. A* **28** 697
- Lee M-T, Michelin S E, Machado L E and Brescansin L M 1993 *J. Phys. B: At. Mol. Opt. Phys.* **26** L203
- Lima M A P, Gibson T L, McKoy V and Huo W M 1988 *Phys. Rev. A* **38** 4527
- Lucchese R R, Raseev G and McKoy V 1982 *Phys. Rev. A* **25** 2572
- Machado L E, Brescansin L M, Lima M A P, Braunstein M and McKoy V 1990 *J. Chem. Phys.* **92** 2362
- Meneses G D, Pagan C B and Machado L E 1990 *Phys. Rev. A* **41** 4740 and references therein
- Middleton A G, Brunger M J and Teubner P J O 1993 *J. Phys. B: At. Mol. Opt. Phys.* **26** 1743
- Parker S D, McCurdy C W, Rescigno T N and Lengsfeld B H III 1991 *Phys. Rev. A* **43** 3514
- Pritchard H P, McKoy V and Lima M A P 1990 *Phys. Rev. A* **41** 546
- Rescigno T N, McCurdy C W and McKoy V 1974 *J. Phys. B: At. Mol. Phys.* **7** 2396
- Schaefer H F III 1977 *Methods of Electronic Structure Theory* (New York: Plenum) p 334
- Trajmar S, Register D F and Chutjian A 1983 *Phys. Rep.* **97** 219